Journal of Neuroendocrinology

Journal of Neuroendocrinology, 2013, **25**, 131–144

ORIGINAL ARTICLE

Sex Steroid Levels and AD-Like Pathology in 3xTgAD Mice

C. R. Overk*[1], S. E. Perez*[1], C. Ma†, M. D. Taves†‡, K. K. Soma†‡[2] and E. J. Mufson*[2]

**Department of Neurological Sciences, Rush University Medical Center, Chicago, IL, USA.*

†Department of Psychology, University of British Columbia, Vancouver, Canada.

‡Department of Zoology, University of British Columbia, Vancouver, Canada.

Journal of Neuroendocrinology

Decreases in testosterone and 17β-oestradiol (E_2) are associated with an increased risk for Alzheimer's disease (AD), which has been attributed to an increase in β-amyloid and tau pathological lesions. Although recent studies have used transgenic animal models to test the effects of sex steroid manipulations on AD-like pathology, almost none have systematically characterised the associations between AD lesions and sex steroid levels in the blood or brain in any mutant model. The present study evaluated age-related changes in testosterone and E_2 concentrations, as well as androgen receptor (AR) and oestrogen receptor (ER) α and β expression, in brain regions displaying AD pathology in intact male and female 3xTgAD and nontransgenic (ntg) mice. We report for the first time that circulating and brain testosterone levels significantly increase in male 3xTgAD mice with age, but without changes in AR-immunoreactive (IR) cell number in the hippocampal CA1 or medial amygdala. The age-related increase in hippocampal testosterone levels correlated positively with increases in the conformational tau isoform, Alz50. These data suggest that the over-expression of human tau up-regulate the hypothalamic-pituitary-gonadal axis in these mice. Although circulating and brain E_2 levels remained stable with age in both male and female 3xTgAD and ntg mice, ER-IR cell number in the hippocampus and medial amygdala decreased with age in female transgenic mice. Furthermore, E_2 levels were significantly higher in the hippocampus than in serum, suggesting local production of E_2. Although triple transgenic mice mimic AD-like pathology, they do not fully replicate changes in human sex steroid levels, and may not be the best model for studying the effects of sex steroids on AD lesions.

Key words: Alzheimer's disease, androgen receptor, estrogen receptor, hippocampus, transgenic mouse, testosterone, oestradiol

doi: 10.1111/j.1365-2826.2012.02374.x

Correspondence to Elliott J. Mufson, Alla V. and Solomon Jesmer Chair in Aging, Rush University Medical Center, 1735 W. Harrison Street, Suite 300, Chicago, IL 60612, USA (e-mail: emufson@rush.edu*).*

[1]These authors contributed equally to this study.

[2]These authors are the co-principal investigators.

Alzheimer's disease (AD), the most common type of the dementia among the elderly, is pathologically characterised by β-amyloid (Aβ) deposition and neurofibrillary tangles (1,2). Although ageing is a major risk factor for AD, there is evidence that decreases in sex steroids, such as testosterone and 17β-oestradiol (E_2), play a role in cognitive decline during ageing and AD in a sex-specific manner (3). In men, there is a gradual reduction in circulating testosterone levels, which is associated with cognitive impairment and increased risk of AD (3). In women, serum E_2 levels decrease during menopause, which precedes cognitive decline and an increased risk of AD. Although controversial, epidemiological and clinical trial studies suggest that sex steroid treatment may prevent age-related cognitive decline and lower the risk of dementia and AD (4).

Testosterone and E_2 bind to their cognate androgen receptors (AR) and oestrogen receptors (ER), respectively. High densities of these receptors are found in areas of the brain that mediate cognition, including the cortex, hippocampus and amygdala (5,6), all of which display extensive AD pathology (1). Despite the presence of steroid receptors and AD lesions in these brain regions, the role that sex steroids play in the development of AD pathology remains unclear. It has been suggested that the disconnection between circulating and brain E_2 levels may underlie cognitive impairment in AD (7).

To determine the role of sex steroids in the development of AD pathology, experimental manipulations of sex steroid levels in animal models of AD have been accomplished by gonadectomy (8–11), crosses with genetic knockouts (7,12) or pharmacological inhibitors

of steroidogenic enzymes (13). Recently, Oddo *et al.* (14) developed a triple transgenic mouse (3xTgAD) harboring the human amyloid precursor protein (APP) Swedish mutation (APP_{swe}), presenilin 1 ($PS1_{M146V}$) and microtubule associated protein tau (Tau_{P301L}). These triple transgenic mutant mice display increases in intraneuroneal and extraneuroneal Aβ and tau in the cortex, hippocampus, amygdala, and brainstem in an age-dependent manner (8,14–18). Decreasing testosterone and E_2 levels via gonadectomy (8–11,19) or inhibiting the production of oestrogens via an aromatase inhibitor (13), alter the deposition of APP/Aβ plaques. Because no studies have measured the endogenous levels of testosterone and E_2 in the serum or brain of 3xTgAD mice, the present study aimed to characterise these hormone levels and determine their associations with the onset of age-related AD-pathology in the brain of these mutant mice.

Here we characterised for the first time levels of testosterone and E_2 in the serum, cortex, hippocampus, amygdala and hypothalamus of 4–6- and 13–14-month-old male and female 3xTgAD and nontransgenic (ntg) mice. Furthermore, we combined immunohistochemistry, densitometry and unbiased stereological counting procedures to quantify the number of AR, ERα and ERβ positive neurones, as well as the amount of AD-like pathology in these areas to determine their interactions with serum and brain sex steroid levels.

Materials and methods

Experimental subjects

A total of 100 young (4–6 months) and older (13–14 months), male and female 3xTgAD and ntg mice obtained from our in-house colony were used in this study. Transgenic and ntg mice breeding pairs were kindly provided by Dr Frank LaFerla from the University of California Irvine (Irvine, CA, USA). These mice were generated using a hybrid 129/C57BL/6 background strain to produce homozygous animals for APP_{swe}, $PS1_{M146V}$ and Tau_{P301L} (14). Up to five mice were single-sex housed in clear plastic cages. Subjects were given *ad lib.* access to standard rodent chow and water and maintained under a 12 : 12 h light/dark cycle. All animal care and procedures were conducted with approved institutional animal care protocols and in accordance with the NIH Guide for the Care and Use of Laboratory Animals. Male and female mice were randomised to each experimental group and randomly chosen for perfusion independent of assigned experimental group (Table 1).

Table 1. Number of Animals and Groups Used for Biochemical and Immunohistochemical Characterisation of 3xTgAD and ntg Mice.

Parameter	Sex	Genotype	Age (months)	n
[E_2] and ER	M	ntg	4–6	6
[E_2] and ER	M	ntg	13–14	5
[E_2] and ER	M	3xTgAD	4–6	6
[E_2] and ER	M	3xTgAD	13–14	6
[E_2] and ER	F	ntg	4–6	6
[E_2] and ER	F	ntg	13–14	6
[E_2] and ER	F	3xTgAD	4–6	6
[E_2] and ER	F	3xTgAD	13–14	6
[T] and AR	M	ntg	4–6	6
[T] and AR	M	ntg	13–14	6
[T] and AR	M	3xTgAD	4–6	6
[T] and AR	M	3xTgAD	13–14	6
[T] and AR	F	ntg	4–6	6
[T] and AR	F	ntg	13–14	6
[T] and AR	F	3xTgAD	4–6	6
[T] and AR	F	3xTgAD	13–14	6

AR, androgen receptor; E_2, 17β-oestradiol; ER, oestrogen receptor; F, female; M, male; ntg, nontransgenic; T, testosterone.

Tissue collection

Because saline perfusion can alter brain steroid concentrations in a rapid, region-specific manner (20), we performed a preliminary study to measured sex steroid levels in brain tissue harvested from animals with or without saline perfusion. Notably, we found that both testosterone and E_2 concentrations were similar in mouse brain tissue independent of saline perfusion (C. R. Overk, S. E. Perez and M. D. Taves unpublished results). Therefore, all mice used in the present study were rapidly perfused with cold saline as described below.

Before perfusion, young and older female mice underwent vaginal swabbing to determine oestrus stage by vaginal cytology (21), and only females in pro-oestrus were sacrificed to ensure the highest levels of circulating testosterone (22) and E_2 (21) and to avoid hormonal variability as a result of cycling. The pro-oestrous stage in vaginal smears was identified by the presence of clusters of round, nucleated epithelial cells, which often have a granular appearance at the light microscope level (21). Additional precautions were taken to avoid stress before sacrifice, including habituating all mice to human handling, maintaining animals in an area separate from the perfusion set-up, and rapid anaesthetisation and perfusion (< 5 min). All mice were deeply anaesthetised with ketamine/xylazine (95 and 5 mg/kg body weight, respectively) and cardiac blood was collected just before transcardial perfusion with ice-cold physiological saline (0.9% NaCl, pH 7.4). Brains were rapidly removed from the calvarium and hemisected. One hemisphere was immersion fixed in a solution consisting of 4% paraformaldehyde and 0.1% glutaraldehyde in 0.1 M phosphate-buffered saline (PBS; pH 7.4) for 24 h at 4 °C and then placed in a cryoprotectant solution composed of 30% sucrose in PBS at 4 °C for at least 24 h. These hemispheres were cut frozen in the coronal plane on a sliding knife microtome at 40 μm thickness into six adjacent series and stored at −20 °C in a cryoprotectant solution (30% ethylene glycol, 30% glycerol, in 0.1 M PBS) before processing.

The other hemisphere was placed in a cold stainless steel brain matrix and cut into 1-mm thick coronal slabs containing the cortex, hippocampus, amygdala and hypothalamus. These four regions were rapidly dissected on wet ice and frozen on dry ice, as described previously (23). Approximately 300 μl of whole blood was centrifuged at 2300 ***g*** units at room temperature for 10 min, the serum was pipetted into a separate 1.5-ml microcentrifuge tube, and both whole blood and serum were stored at −80 °C before analysis.

Immunohistochemistry and immunofluorescence

Free-floating sections were immunohistochemically processed using antibodies directed against APP/Aβ (6E10; dilution 1 : 2000; Covance, Princeton, NJ, USA) (13,17) and the tau conformational 66-kDa protein, Alz50 (dilution 1 : 10 000) (17) or mounted on charged slides and boiled in citric acid (pH 8.5) for 20 min before incubation with antibodies directed against ERα (dilution 1 : 500; lot number 1151207; Leica, Newcastle, UK) or ERβ (dilution 1 : 200; Z8P Zymed Labs, San Francisco, CA, USA), as reported previously (24), or AR (dilution 1 : 1000; PG21 catalogue number 06–680; Millipore,

Billerica, MA, USA). Peroxidase avidin-biotin was used to amplify and visualise the different antigen signals using procedures established in our laboratory (23). After incubation with the appropriate biotinylated secondary antibody and the application of Vectastain ABC kit (Vector Labs, Burlingame, CA, USA), immunoreactions were revealed using diaminobenzidine (DAB; Sigma, St Louis, IL, USA) with or without nickel intensification. Immunohistochemical controls have been reported previously for 6E10 (17), Alz50 (17), ERα (24), ERβ (24) and AR (25). Additional sections were double immunolabelled for AR and Alz50 in accordance with our previously published protocol (23). This dual staining resulted in an easily identifiable two-coloured profile: blue for AR-positive and brown for Alz50-positive profiles at the light microscopic level. Some sections were counterstained with cresyl violet to aid in cytoarchitectonic evaluation. Anatomical nomenclature was according to the atlas of Paxinos and Franklin (26). Photomicrographs were obtained with the aid of a Nikon Eclipse 80i microscope (Nikon, Tokyo, Japan).

Additional sections from the same cases were double-labeled for 6E10 and AR using immunofluorescence. Tissue was washed in phosphate buffer, mounted on charged slides before citric acid antigen retrieval (see above) and incubated with anti-AR (dilution 1 : 50) in a humidifying chamber. Sections were then rinsed and incubated in a secondary antibody (Cy2; dilution 1 : 200; Jackson ImmunoResearch, West Grove, PA, USA) for 120 min in the dark. Sections were washed with TBS containing 5% goat serum and then incubated with 6E10 (dilution 1 : 100) overnight in the dark and then rinsed and incubated in a different secondary antibody (Cy3; dilution 1 : 300; Jackson ImmunoResearch) for 120 min in the dark. Immunofluorescence was visualised using a Zeiss Axioplan 2 microscope (Carl Zeiss, Oberkochen, Germany) using excitation filters at wavelengths 489 and 555 nm and emission filters at 505 and 570 nm for Cy2 and Cy3, respectively. Fluorescent images were stored on a computer and contrast was enhanced using ADOBE PHOTOSHOP, version 7 (Adobe Systems, San Jose, CA, USA).

Densitometry

Hippocampal tissue immunostained with 6E10 and Alz50 antibodies from male young (n = 12) and older (n = 11) and female young (n = 6) and older (n = 5) 3xTgAD mice were used to measure the relative age-related changes in APP/Aβ and tau expression in CA1 pyramidal neurones by optical densitometry (OD) using Scion Image, version 1.60 (Scion, Frederick, MD, USA) as described previously (27,28). Briefly, every sixth section (separated by 240 μm) was analysed using a × 40 objective, centering the camera over the pyramidal layer of the CA1 field. The captured frame was manually outlined from an average of nine to ten sections from each animal to obtain the OD measurements in CA1 pyramidal neurones. The OD measurements were automatically analysed in grey-scale images. Five ODs from regions of the hippocampus devoid of 6E10 or Alz50 immunostaining were measured, averaged and subtracted from the final 6E10 and Alz50 OD values. Previous studies have shown that OD measurements reflect changes in protein expression, which parallel those obtained using a biochemical protein assay (28,29).

Stereology procedures

Optical fractionator

Stereological methods were used to estimate the number of APP/Aβ-, Alz50-, ERα-, ERβ- and AR-immunoreactive (-IR) profiles utilising an optical fractionator unbiased sampling design (17,27). Immunoreactive neurones were only counted if the first recognisable profile came into focus within the counting frame. This method allowed for a uniform, systematic and random design. Focusing through the z-axis revealed that each antibody penetrated the full depth of each section. Section thickness was determined at each site by focussing on the top of the section, zeroing the z-axis and focussing on the bottom of the section. The dissector height was based on section thickness for each case with at least a 1 μm top and bottom guard zone. The forbidden zones were never included in the cell counting.

Optical fractionator parametres for estimating the number of ERα-positive hippocampal CA1 neurones were: perikarya within sections separated by approximately 240 μm were outlined using a × 10 objective attached to a Nikon Optihot-2 microscope. A systematic sampling of the outlined areas was made from a random starting point using STEREOINVESTIGATOR, version 8.21.1 (Micro-BrightField, Cochester, VT, USA). Counts were taken at predetermined intervals (x = 150, y = 150), and a counting frame (107 × 107 μm = 11 440 μm^2) was superimposed on the live image of the tissue sections. Sections were analysed using a × 60 PlanApo oil immersion objective with a 1.4 numerical aperture. The average Gunderson coefficient of error, m = 1 (30), was 0.09. Average section thickness across all groups was 13.9 μm.

Hippocampal CA1 neurones that were immunopositive for AR were counted in every twelfth section (480 μm) using a counting frame (30 × 30 μm) and sampling grid size (166 × 114) for both males and females. The average coefficient of error was 0.08 with an average tissue thickness of 20.4 μm.

ERα-IR cells in the medial amygdala were counted in every sixth section (240 μm) using a counting frame (130 × 90 μm) and sampling grid size (240 × 240 μm) for both males and females. The average coefficient of error was 0.07 with an average tissue thickness of 13.4 μm.

ERβ-IR profiles in the medial amygdala were counted in every sixth section (240 μm) using a counting frame (36 × 36 μm) and sampling grid size (58 × 58 μm) for both males and females. The average coefficient of error was 0.13 with an average tissue thickness of 6.3 μm.

APP/Aβ-IR hippocampal CA1 neurones were counted in every sixth section using a counting frame (30 × 30 μm) and sampling grid size (101 × 161) for both males and females. The average coefficient of error was 0.066 ± 0.008 with an average tissue thickness of 12.4 μm.

Alz50-IR pyramidal neurones in the CA1 layer of the hippocampus were counted in every sixth section using a counting frame (90 × 90 μm) and sampling grid size (200 × 200 μm) for both males and females. The average coefficient of error was 0.07 with an average tissue thickness of 12.1 μm.

Plaque area and number

The area fraction fractionator stereological probe was used to determine the area/plaque load occupied by 6E10-IR plaques in the subiculum. The subiculum was outlined in sections 240 μm apart extending from its dorsal–rostral location to its more ventral–caudal portion. Because 3xTgAD mice develop Aβ-plaques primarily in the subiculum around 9 months of age, only the 13–14-month-old cohorts were evaluated in the present study. Subicular 6E10 plaque load was determined using a counting frame of 80 × 80 μm, a sampling grid (220 × 220) and a grid space of 7 μm. In addition, the number of APP/Aβ-IR plaques in the subiculum was counted manually using a Nikon Eclipse 80i scope with a × 20 objective and a × 10 ocular magnification.

Serum and brain steroid levels

Solid phase extraction (SPE) was performed before quantifying testosterone and E_2 levels in serum and brain (31). SPE extracts steroids from the serum and tissue and removes substances that may interfere with the assays. This is crucial when measuring sex steroid concentrations in small samples, particularly for E_2 (32). Stringent sample preparation eliminated the need to pool samples and enabled correlations between steroid levels and steroid receptors within individuals. Moreover, correlations at the individual subject level were possible as a result of the use of hemisected brains, where one hemisphere was used for steroid analysis and the other hemisphere was used for histopathological analysis.

SPE

One set of subjects was used to measure testosterone, and another set of subjects was used to measure E_2 (Table 1). Steroids were extracted from all samples (serum, whole blood, and brain) using SPE with C_{18} columns and employing a modification of a previously published method (33). This procedure provides high and consistent steroid recoveries. Whole blood and brain samples were homogenised in ice-cold deionised water and then high-performance liquid chromatography (HPLC)-grade methanol was immediately added. Samples were incubated overnight at 4 °C. Samples were then centrifuged and supernatants (up to a maximum of 1 ml) were diluted with 10 ml of deionised water to prepare for loading onto C_{18} columns. Serum samples were similarly diluted with 10 ml of deionised water. C_{18} columns were primed with 3 ml HPLC-grade ethanol, equilibrated with 10 ml of deionised water, and samples were loaded. Samples were then washed with 10 ml of 40% methanol to remove interfering substances, such as brain lipids. Steroids were eluted with 5 ml of 90% HPLC-grade methanol and dried at 40 °C in a vacuum centrifuge (ThermoElectron SPD111V Speedvac; Thermo Fisher Scientific Inc., Waltham, MA, USA). Dried extracts were resuspended with assay diluent containing absolute ethanol (1% of total volume) to aid in the suspension of steroids (33).

To calculate steroid recovery, we spiked aliquots of serum or brain tissue with known amounts of testosterone or E_2, and compared steroid amounts in spiked and unspiked samples. Testosterone and E_2 recoveries were high (i.e. close to 100%) and consistent (Table 2), and samples were corrected for recovery using the average recovery values in Table 2. We also evaluated the ability of the SPE protocol to remove interfering substances by serially diluting serum and brain samples (Fig. 1). Displacement curves were parallel to the standard curve (Fig. 1), indicating the effective removal of interfering substances (31). We were able to measure E_2 in serum but not in whole blood (incomplete removal of interfering substances from whole blood samples).

Radioimmunoassays

Samples were assayed for either testosterone or E_2 using sensitive and specific radioimmunoassays (RIAs) that we validated for use with mouse brain (31). Testosterone was measured in duplicate using a double-antibody ^{125}I RIA (#07189102; MP Biomedicals, Solon, OH, USA) that was modified to increase sensitivity. Briefly, 200 μl of primary antibody was added to 175 μl of sample and then incubated for 4 h at room temperature. Next, 200 μl of tracer was added, and samples were incubated overnight at room temperature. Then 50 μl of secondary antibody (precipitant) was added, and tubes were incubated for 60 min in a water bath at 37 °C with shaking at 90 r.p.m.. Finally, tubes were centrifuged at 2383 ***g*** units for 30 min at 4 °C, supernatants were decanted, and analysed using a gamma counter for 1 min each. These modifications resulted in a detection limit of 0.31 pg testosterone/tube and also allowed more samples to be measured per kit (over two-fold decrease in cost per sample). The testosterone antibody has low cross-reactivity with 5α-dihydrotestosterone (3.40%), 5α-androstanediol (2.20%), 5β-androstanediol (0.71%), androstenedione (0.56%), dehydroepiandrosterone and oestrogens (< 0.01%), as reported by the manufacturer. Water blanks (n = 15 total) were extracted and assayed along with all tissue samples, as negative controls; nine were not detectable and six were just above the lowest point on the standard curve. As a positive control, known amounts of testosterone in assay buffer (n = 16 total) were also processed along with tissue samples, resulting in an average recovery of 116 ± 2%. All tissue samples had detectable amounts of testosterone. Intra-assay variation was 6.7% and inter-assay variation was 5.8%.

E_2 was measured using a modified double-antibody ^{125}I RIA (Beckman Coulter; DSL-4800, Chino, CA, USA) as described previously (34,35). The detection limit was 0.20 pg E_2/tube. Samples were measured as singletons, to allow quantification of low E_2 concentrations (34). Water blanks (n = 11 total) and known amounts of E_2 (n = 5 total) were processed in parallel with all tissue samples. Eight water blanks were not detectable, and three were just above the lowest point on the standard curve. Recovery of E_2 standards in assay buffer was 109 ± 4%. Intra-assay variation was 7.2% and inter-assay variation was 7.7%.

Table 2. Recovery of Testosterone and 17β-Oestradiol from Mouse Serum and Brain.

	Serum	Brain
Testosterone		
Unspiked samples (pg/tube)	24.9 ± 0.5 (n = 5)	1.2 ± 0.1 (n = 5)
Spiked samples (pg/tube)	32.8 ± 0.7 (n = 5)	9.0 ± 0.1 (n = 5)
Spike amount (pg/tube)	8.8	7.3
Recovery	90%	108%
17β-oestradiol		
Unspiked samples (pg/tube)	0.00 ± 0.00 (n = 5)	0.76 ± 0.05 (n = 13)
Spiked samples (pg/tube)	0.70 ± 0.01 (n = 5)	1.44 ± 0.06 (n = 13)
Spike amount (pg/tube)	0.72	0.66
Recovery	97%	103%

Pools of mouse serum and homogenised brain tissue were divided into aliquots. Testosterone or oestradiol was added to some aliquots ('spiked samples') but not other aliquots ('unspiked samples'). 'Spike amount' is the known amount of testosterone or oestradiol that was added to spiked samples. The observed difference between spiked and unspiked samples was compared with the expected difference (the spike amount), and this is presented as 'recovery.' Oestradiol was nondetectable in unspiked samples from this particular pool of serum, and so the values were set to zero.

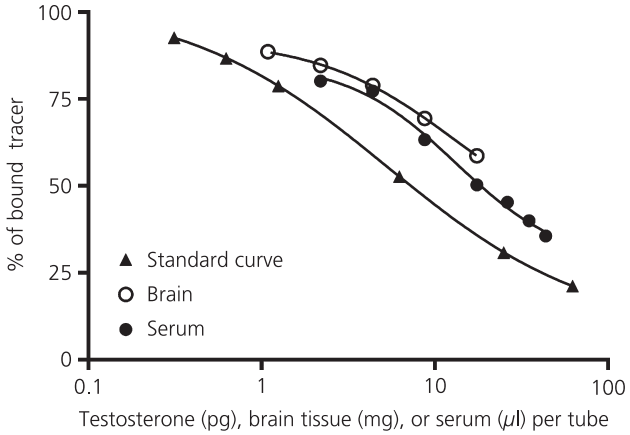

Fig. 1. Serial dilution of mouse serum and brain. The parallelism between the diluted samples and the testosterone standard curve demonstrates that the stringent sample preparation employing solid phase extraction (SPE) effectively removes interfering substances from the samples. These data and previous data clearly indicate that SPE, when combined with extensive washes, allows for measurement of steroids in lipid-rich brain samples and serum from mice.

Statistical analysis

Male and female data from testosterone and E_2 levels, as well as AR and ER cell counts, were separately evaluated with two-way ANOVAS (factors: age and genotype) followed by Holm–Sidak post-hoc tests for multiple

comparisons or with nonparametric Kruskal–Wallis tests for data without Gaussian distribution after Neperian logarithm normalisation (Sigma Stat 3.5; Systat Software, Inc., San Jose, CA, USA). Data from APP/Aβ and Alz50 cell counts, plaque load, as well as Alz50 and APP/Aβ OD measurements, were statistically evaluated with two-way ANOVAS (factors: age and sex) or with Kruskal–Wallis tests followed by post-hoc tests, as appropriate. Regional differences in E_2 levels were statistically examined with Friedman repeated measures followed by Tukey tests to identify pairwise differences. Correlations were performed with Spearman tests. $P < 0.05$ (two-tailed) was considered statistically significant. The data were graphically represented using the mean ± SEM (Sigma Plot 10.0; Systat Software, Inc.).

Results

Hippocampal plaque and tau pathology increases with age in a sex-dependent manner in 3xTgAD mice

Hippocampal plaque and neurofibrillary tangle pathology was found only in 3xTgAD mice. In the hippocampus, 6E10 and Alz50 antibodies were used to visualise APP/Aβ positive neurones/plaques and intraneuroneal conformational tau, respectively. As reported previously (18), 6E10-IR plaques were virtually absent in young (4–6 months) 3xTgAD mice (Fig. 2A,D). In agreement with previous observations (14,15,19), we found a sex-dependent increase in extraneuroneal Aβ deposition in the hippocampus of older (13–14 months) 3xTgAD mice (Fig. 2A–F). Specifically, the area of the hippocampal/subicular complex occupied by 6E10-IR plaques was significantly greater in older females than older males (Fig. 2C; $P < 0.01$). Additionally, the raw number of 6E10-IR plaques was significantly higher in older females than older males (Fig. 2F; $P < 0.01$).

OD measurements of 6E10-IR hippocampal CA1 pyramidal neurones revealed a significant interaction between sex and age ($P = 0.001$). Specifically, 6E10-IR OD measurements increased with age in males (Fig. 2G–I; Holm-Sidak method, $P < 0.05$) but decreased with age in females (Fig. 2I; Holm-Sidak method, $P < 0.05$). CA1 neurone OD measurements for 6E10-IR were significantly higher in young females than young males (Fig. 2I; Holm-Sidak method, $P < 0.05$).

OD measurements of Alz50-IR CA1 pyramidal neurones were significantly higher in older males than young males but unchanged with age in females (Fig. 2J–L; Holm-Sidak method, $P < 0.05$). Furthermore, Alz50-IR OD measurements in CA1 pyramidal neurones were significantly higher in older male than female mice (Fig. 2L; Holm-Sidak method, $P < 0.05$).

Testosterone but not E_2 levels increased in serum and brain with age in male 3xTgAD mice

We measured testosterone levels in serum, cortex, hippocampus, amygdala and hypothalamus from male and female, young and older 3xTgAD and ntg mice (Fig. 3A–H). Unexpectedly, testosterone levels in serum (Fig. 3A) and each brain region examined (Fig. 3B–E) were higher in older compared to young male 3xTgAD mice ($P < 0.05$ in all cases). By contrast, there were no significant changes in serum or brain testosterone levels across ages in ntg males (Fig. 3A–E). Furthermore, there were significant differences in testosterone concentrations in both the serum and brain between older 3xTgAD and older ntg male mice (Fig. 3A–E; $P < 0.05$ in all cases). There were similar age- and genotype-dependent changes in testosterone concentrations in whole blood samples (data not shown). On the other hand, females showed a trend toward decreased levels of testosterone with age in serum (Fig. 3F), the hippocampus and the hypothalamus in both genotypes ($P > 0.05$), which only reached significance in the cortex of ntg mice (Fig. 3G; $P < 0.05$) and the amygdala of 3xTgAD mice (Fig. 3H; $P < 0.05$).

There were no significant effects of age on E_2 levels in serum or brain samples across all groups ($P > 0.05$, data not shown). Collapsing groups by age revealed that E_2 levels were consistently higher in the hippocampus and amygdala than in the cortex and serum, regardless of sex or genotype (Fig. 4A–D; Friedman repeated measures, $P < 0.05$ in all cases).

Oestrogen receptor, but not androgen receptor, decreased in a region-, sex-, age- and genotype-dependent manner

The number of ERα-, ERβ- and AR-positive cells was counted in the hippocampus and medial amygdala, which are two regions affected by AD pathology in 3xTgAD mice (Fig. 5). In the hippocampus, the number of ERα-IR cells was significantly decreased in older females, independent of genotype (Fig. 5A–C; $P < 0.05$). Specifically, in the medial amygdala, the number of ERα-IR cells was significantly decreased in 3xTgAD females, independent of age (Fig. 5D–F). The number of ERβ-IR neurones in the medial amygdala of females was decreased with age, independent of genotype (Fig. 5G–I). ERβ-IR cells were not visualised in the hippocampus similar to the findings of previous studies in rodents (24,36,37). Furthermore, there were no significant differences in ERα-IR or ERβ-IR cell number with age in male 3xTgAD and ntg mice. Because there are almost no ER positive neurones in the cortex, we chose not to analyse this region for changes in immunodensity. With regard to the hypothalamus, we did not evaluate this region because it does not display AD-like pathology in our transgenic mice.

The number of AR-IR neurones in males was unaffected by either genotype or age in the hippocampus (Fig. 5J,L) or medial amygdala (Fig. 5K,M). Androgen receptor immunostaining in female mice in both structures was below immunohistochemical detectable levels needed for quantitation.

Co-localisation of 6E10-IR and Alz50-IR with AR-IR in hippocampal CA1 neurones

Double immunofluorescence and bright field immunohistochemistry were carried out to co-localise AR with 6E10 (Fig. 6A–C) or Alz50 (Fig. 6D) in the hippocampus of older male 3xTgAD mice. Although almost all CA1 neurones displayed both 6E10 and AR-IR (Fig. 6C), a few neurones were AR positive but 6E10 immunonegative (Fig. 6A–C). Similarly, all Alz50-IR CA1 pyramidal neurones were also positive for AR-IR (Fig. 6D).

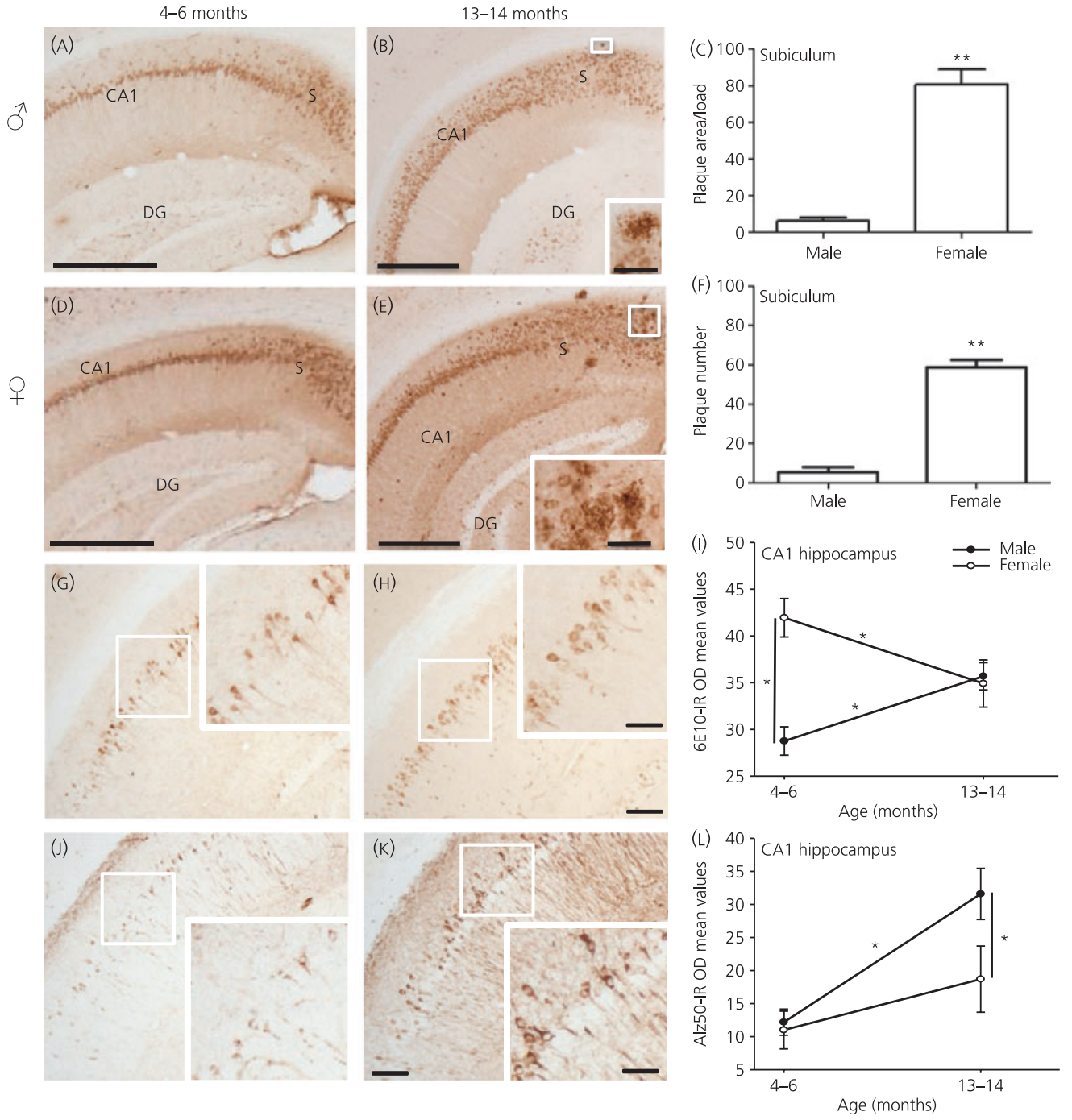

Fig. 2. Photomicrographs of 6E10 (Aβ/APP) immunostaining showing a virtual absence of plaques in male (A) and female (D) hippocampus in young (4–6 month-old) 3xTgAD mice. Aged males (B) displayed less plaque pathology compared to age-matched female (E) 3xTgAD mice. Insets show higher magnification images of 6E10 positive plaques outlined by a small white box in the subiculum of an old male (B) and female (E) mutant mouse. Histograms show a significant increase in subicular plaque load (C) and number (F) in female 13–14-month-old mice compared to age-matched male mutant mice. Photomicrographs show 6E10- and Alz50-positive CA1 hippocampal neurones in young (G, J) and old (H, K) 3xTgAD mice. Note the increase in immunolabelling between the young and old mutant mice. Insets show a higher magnification image of intraneuroneal 6E10 and Alz50 staining outlined in (G, H) and (J, K), respectively. Linear graphic representation of optical density (OD) measurements of 6E10 positive neurones showing a significant increased between young females compared to young males (I), whereas the OD measurements for Alz50 immunostaining were significantly increased in older males compared to young male 3xTgAD mice (L). Scale bars (A, B, D, E) = 500 μm; insets in (B) and (E) = 50 μm. Scale bars (G, H, J, K) = 100 μm; insets = 50 μm. CA1, hippocampal CA1 field; DG, dentate gyrus; S, subiculum. *P < 0.05; **P < 0.01.

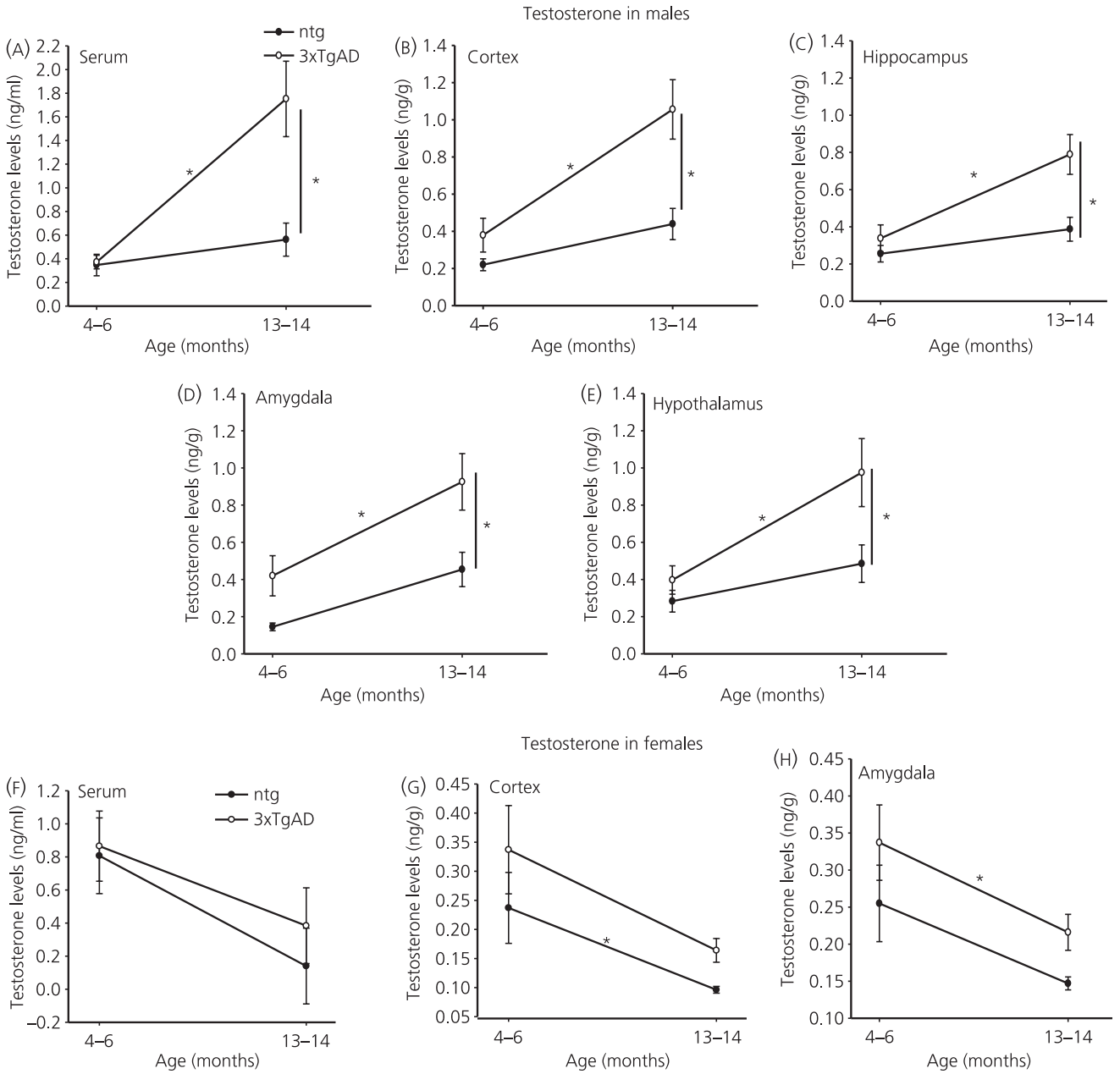

Fig. 3. Linear graphic representation showing an increase in testosterone levels in serum (A) and across brain regions (B–E) with age in male but not female (F–H) 3xTgAD mice. Note the trend towards a decrease in testosterone levels with age in serum (F) and cortex (G) in female 3xTgAD, reaching significance only in the amygdala (H). *$P < 0.05$. ntg, Nontransgenic.

Age-related increase in number of hippocampal CA1 6E10- and Alz50-IR neurones in male 3xTgAD mice

Stereological counts of hippocampal CA1 6E10- and Alz50-IR neurones were determined in an adjacent series of sections to those used for the estimation of the number of AR-positive cells. There was a significant increase in the number of CA1 6E10-IR cells with age in male ($P < 0.01$) but not in female 3xTgAD mice (Fig. 6E). On the other hand, the number of Alz50-IR cells increased in both male ($P < 0.01$) and female ($P < 0.05$) 3xTgAD mice with age (Fig. 6F). All CA1 neurones that were 6E10-IR or Alz50-IR were also AR-positive in aged male 3xTgAD. The estimated number of CA1 pyramidal neurones co-expressing 6E10 and AR was approximately 46%, whereas the percentage of profiles co-expressing Alz50 and AR was 15% of the total population of AR-positive neurones.

In addition, we correlated testosterone concentration with AD neuropathology in male 3xTgAD mice. Notably, hippocampal testosterone concentrations correlated positively with hippocampal CA1 and Alz50 OD measurements (Fig. 6G; Spearman correlation coefficient = 0.594, $P = 0.037$) but not with 6E10 OD values or

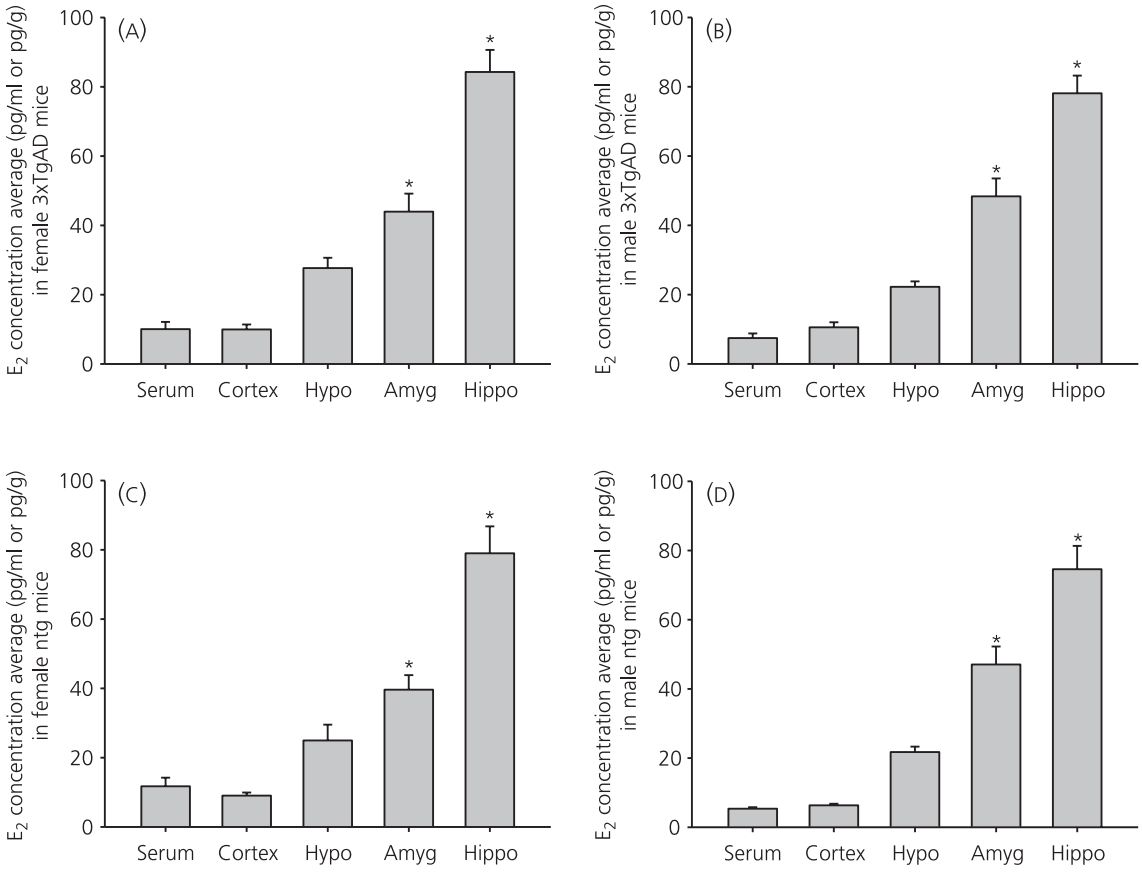

Fig. 4. Histograms showing brain region-dependent 17β-oestradiol (E_2) concentrations in male and female 3xTgAD and nontransgenic mice independent of age. E_2 levels were significantly increased in the amygdala (Amyg) and hippocampus (Hippo) but not in the hypothalamus (Hypo) compared to either cortex or serum levels (repeated measures one-way ANOVA, *$P < 0.05$).

number of neurones containing these markers in male 3xTgAD mice. This observation indicates that local testosterone levels and Alz50 neurone protein expression tend to increase concurrently with age in male 3xTgAD mice.

Discussion

The present study evaluated age-related changes in testosterone and E_2 concentrations and their respective cognate receptors in select brain regions that display AD-like pathology in intact male and female 3xTgAD mice. We report for the first time that circulating and brain testosterone levels were significantly increased in male 3xTgAD mice with age, without corresponding changes in AR-IR neurone number in either the CA1 region of the hippocampus or medial amygdaloid nucleus. Interestingly, the hippocampal age-related increase in testosterone correlated positively with an increase in the expression of the early tau pathological conformational marker Alz50. Conversely, although circulating and brain E_2 levels remained stable with age in both male and female 3xTgAD and ntg mice, the number of ER positive hippocampal CA1 and medial amygdala neurones decreased with age in female mice. Additionally, hippocampal E_2 levels were significantly higher than serum E_2 levels in male and female triple transgenic and ntg mice, suggesting local E_2 production. These data point to a possible interaction between tau and testosterone in aged male triple transgenic mice, which may be associated with a sex-specific dysregulation of the hypothalamic-pituitary-gonadal axis.

Testosterone and AR in male 3xTgAD mice

In the present study, we characterised for the first time testosterone concentrations in the serum and brain of young and older 3xTgAD mice and ntg (hybrid 129/C57BL/6) mice. Interestingly, we found similar serum testosterone concentrations in young 3xTgAD and young ntg male mice (approximately 0.4 ng/ml), whereas serum testosterone levels were four-fold higher in older 3xTgAD (approximately 1.75 ng/ml) than older ntg male mice (approximately 0.5 ng/ml). We have found no published studies that measured serum testosterone levels in this particular hybrid mouse strain (129/C57BL/6). The present levels of serum testosterone in ntg male mice are similar to those reported in 3 month-old male CD-1 mice (approximately 0.44 ng/ml) (38) and in adult male C57BL/6J mice (approximately 0.5 ng/ml) (39). There is wide variation in reported testosterone levels for C57BL/6 mice, including higher as well as low testosterone levels (39–42), similar to the low levels found in our mice, suggesting great variability of testosterone in this strain

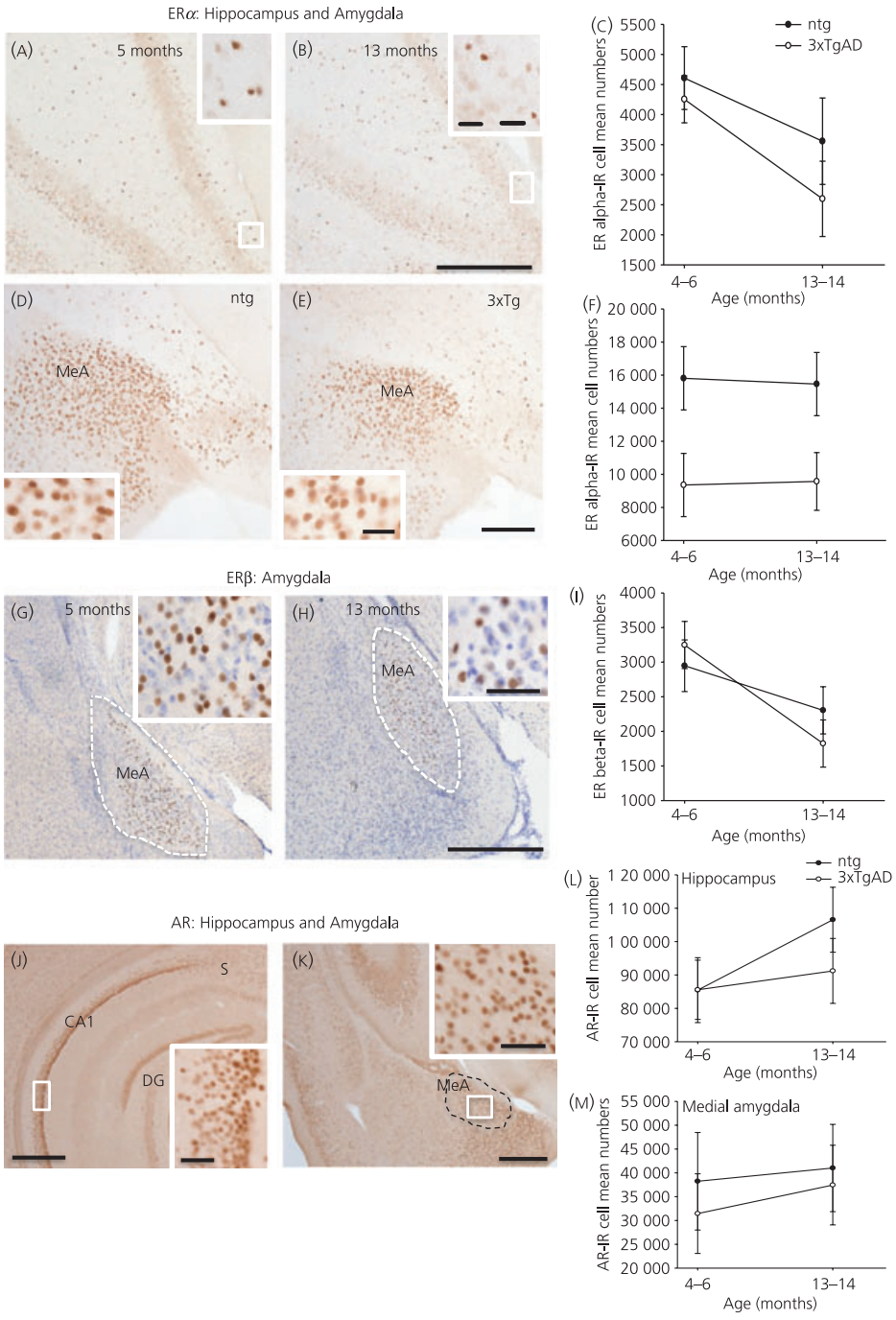

Fig. 5. Photomicrographs showing oestrogen receptor (ER)α positive profiles in the hippocampus of young (A) and old (B) female mutant and within the medial amygdala in female nontransgenic (ntg) (D) and 3xTgAD (E) mice. Insets display high-power images of small-boxed areas in (A) and (B) showing examples of ERα positive profiles. Histograms demonstrating a significant age-related decrease in the number of ERα-positive profiles in the hippocampus (C) independent of genotype. Quantitation revealed significantly fewer ERα–immunoreactive neurones in the medial amygdala of 3xTgAD compared to ntg mice, independent of age (F). Photomicrographs showing a reduction of ERβ positive profiles (brown) within the medial amygdala with age between young ntg (G) and older (H) female 3xTgAD mice. Insets (G, H) show high-power images of ERβ positive neurones within the medial amygdala nucleus (outlined area). (G, H) Tissue was counterstained with cresyl violet, showing blue cellular profiles. Statistical analysis revealed that ERβ-positive cells in the medial amygdala decreased with age, independent of genotype (I). Images showing the distribution of AR-IR profiles in the hippocampus (J) and medial amygdala (K) in an older male 3xTgAD mouse. Insets show high-power images of boxed areas in (J) and (K) indicating AR positive neurones. No age-related change in AR-IR number in male 3xTgAD and ntg as shown graphically in the hippocampus (L) or medial amygdala (M). Scale bars (A, B, D, E) = 200 μm; insets = 30 μm; (G, H) = 250 μm; and insets = 40 μm; (J, K) = 500 μm; insets = 50 μm. CA1, hippocampal CA1 field; DG, dentate gyrus; MeA, medial amygdala; S, subiculum. *$P < 0.05$.

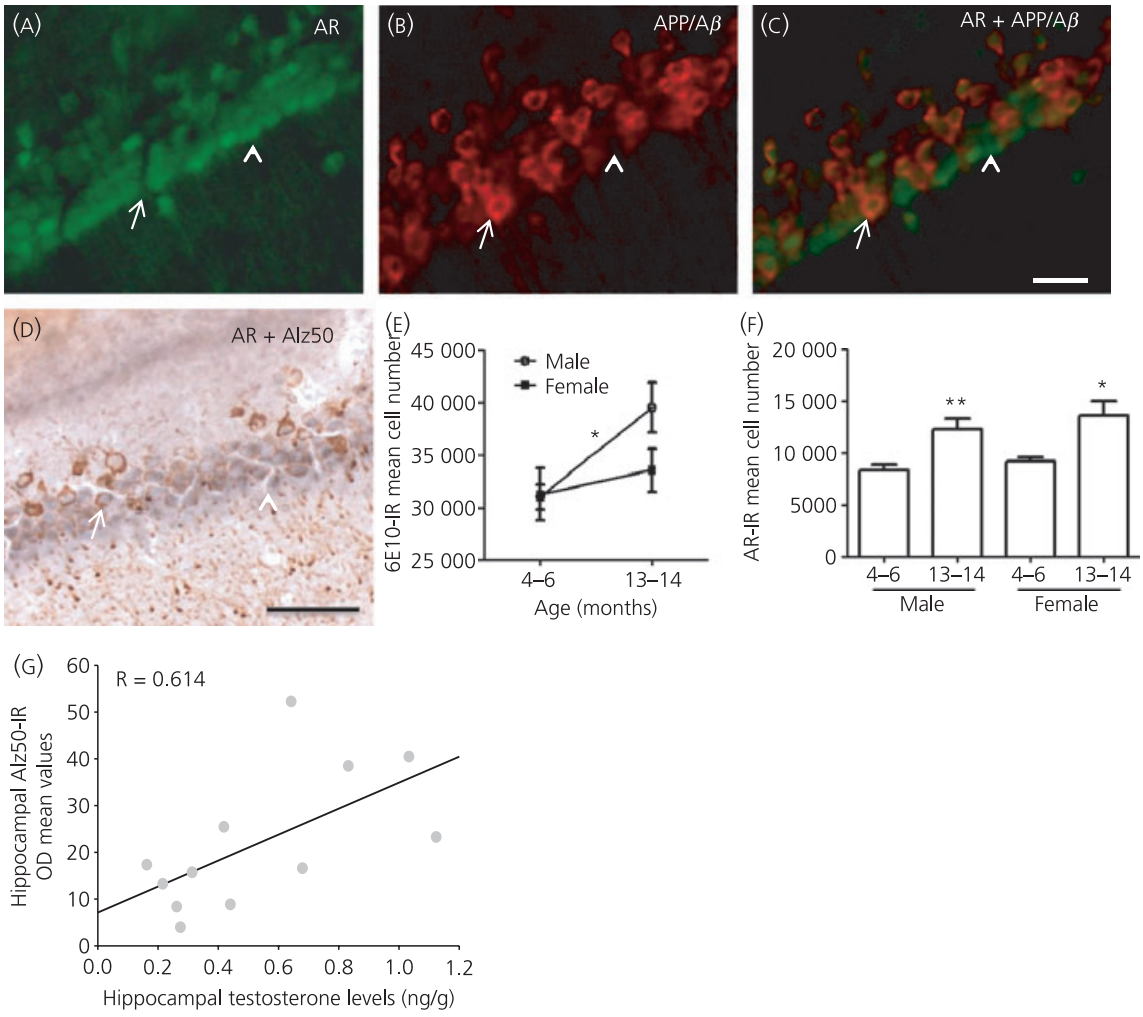

Fig. 6. Co-localisation of androgen receptor (AR) with 6E10 using dual immunoflouresence (A–C) and with Alz50 (D) using bright field microscopy in older triple transgenic mice. Note that all of 6E10 (APP/Aβ) and Alz50 positive cells expressed AR (white arrows) but not all AR neurones were 6E10 or Alz50 positive (white arrowheads). In the hippocampus, the number of 6E10-IR neurones increased significantly in males with age (E) but not females. Both males and females exhibited a significant increase in the number of Alz50-positive cells in hippocampus with age (F). Hippocampal testosterone levels correlated significantly with optical density (OD) measurements for Alz50 (G). Scale bars (A–D) = 50 μm. **P < 001; *P < 0.05.

of mouse. Indeed, it is well-known that testosterone levels vary greatly across mouse strains (43) and several studies have demonstrated that C57BL (6 and 10J) mice display comparatively low T levels (44,45). Because the 3xTgAD mice were generated against a 129 and C57BL/6 hybrid background, it is likely that this mix of strains contributed to the relatively low serum testosterone levels measured here.

Although lower serum testosterone levels have been reported in patients with AD compared to healthy aged male controls, we found a significant age-related increase in testosterone concentrations in serum and brain in male 3xTgAD mice. Conversely, McAllister *et al.* (12) demonstrated a gradual age-related decrease in serum and brain testosterone levels in C57BL/6 ntg and APP_{swe} male mice, suggesting a possible strain or transgene interaction. Interestingly, the increase in testosterone levels in the serum and brain in aged male 3xTgAD mice, which display an age-related plaque and tangle-like pathology in the hippocampus and amygdala (14,15), does not mimic the findings in humans showing that low circulating testosterone is associated with an increased risk for AD in men (19,46). These observations are of particular note because many reports of sex steroid manipulations, including surgical (11,19), pharmacological (13) and genetic approaches (7), performed in transgenic models of AD, failed to establish changes in baseline hormonal levels with age both within and between genotypes.

Similar to other studies, we found that serum testosterone levels were recapitulated in the brain in young and older mice, independent of genotype, supporting the concept that testosterone is synthesised in the periphery and transported to the brain. Paralleling serum concentrations, testosterone levels were consistently increased with age across the different brain regions examined, regardless of the presence or absence of plaque or tangle pathology in these regions. Brain testosterone concentrations in aged mutant males ranged from 0.8 to 1.0 ng/g, and displayed a 2.3-fold increase compared to testosterone levels in young 3xTgAD males,

which ranged from 0.3 to 0.4 ng/g. Nevertheless, the increase in testosterone, the precursor of E_2, was not associated with a concomitant increase in serum or brain E_2 in aged mutant male mice, suggesting that the mechanism(s) involved in the elevated testosterone levels do not translate into higher E_2 levels via aromatisation. Consequently, the effects of testosterone are probably not mediated by the indirect activation of oestrogen signalling pathways in male 3xTgAD. Furthermore, because plaque and tangle-like pathologies are increased in the hippocampus and amygdala with age in the triple transgenic mouse (14,15,18) and both structures are components of a limbic-hypothalamic-pituitary pathway, we suggest that an age-related increase in testosterone is indicative of an alteration in this chemoanatomical system. Dysregulation of this axis may affect gonadotrophin-releasing and luteinising hormone production, which, in turn, affects brain tau conformational and phosphorylation events. Interestingly, neurofilament proteins are found in Leydig cells in testicular tissue in rodents (47), which produce testosterone in the presence of luteinising hormone. It is possible that the mutated tau transgene inserted into the 3xTgAD mouse triggers an up-regulation of testosterone or induces an increase in Leydig cell number in these mutant mice. However, the mechanism by which the overexpression of tau up-regulates testosterone in intact 3xTgAD mice is unknown. Further studies are needed to examine whether other hormones affect this limbic-hypothalamic-pituitary-gonadal pathway, the presence of tau pathologic lesions in testicular tissue in male 3xTgAD mice, and whether there are physiological and behavioral repercussions associated with this age-dependent increase of testosterone in this animal model of AD.

In men, testosterone replacement therapy and high free testosterone levels are associated with improved verbal and spatial memory (48) and a reduced risk of AD (49), suggesting a neuroprotective effect of testosterone against AD pathogenesis. Furthermore, chemical castration for the treatment of prostate cancer is associated with increased levels of Aβ pathology (50). In this regard, we found that the increase in testosterone in aged male 3xTgAD mice was associated with a reduction in hippocampal APP/amyloid plaque pathology compared to age-matched female transgenic mice, perhaps indicative of a neuroprotective effect of testosterone or its involvement in amyloid processing. In this vein, *in vitro* studies have shown that testosterone reduces Aβ levels by altering APP processing toward a non-amyloidogenic pathway and increases the expression of neprilysin, an enzyme involved in Aβ degradation (51). Castration of male 3xTgAD mice increases Aβ deposits in the hippocampus and amygdala and worsens working memory (19). Treatment with testosterone or its metabolite dihydrotestosterone prevents Aβ accumulation in gonadectomised male 3xTgAD mice (11), suggesting that testosterone regulates Aβ pathology. Interestingly, crossing APP23 mutant mice with an aromatase knockout mouse (i.e. APP23/Ar$^{+/-}$) results in low aromatase activity, high levels of serum and brain testosterone and a reduction of Aβ plaques, which is associated with a down-regulation of β-secretase and an up-regulation of neprilysin (7). These findings indicate that testosterone is protective against AD pathology via an E_2-independent pathway (12) and that the age-related increase in hippocampal testosterone underlies the differential Aβ production between male and female 3xTgAD mice. Unexpectedly, hippocampal testosterone concentrations correlated positively with an increase in hippocampal intraneuroneal tau but not with APP/Aβ protein expression, nor hippocampal 6E10- or Alz50-IR cell number.

By contrast to their effects on APP/Aβ, testosterone treatments have been associated with hyperphosphorylated tau prevention (11) via inhibition of glycogen synthase kinase 3β (an enzyme involved in the tau phosphorylation) (52). Therefore, we speculate that age is a major risk factor driving the increase in both testosterone and conformational Alz50 tau isoform expression in male 3xTgAD mice. It is possible that these actions occur through an interaction between tau and ARs, which are highly expressed in CA1 neurones of the hippocampus and co-localise with Alz50. On the other hand, although testosterone levels increased significantly in male mice, the number of AR-positive cells did not change in the hippocampus or medial amygdala with age or genotype. Whether AR receptor expression or changes in receptor affinity are affected by the increase of peripheral circulating and brain testosterone levels is unknown. However, because testosterone is neuroprotective at physiological levels via the AR receptor (53), perhaps increased testosterone production occurs in response to toxic amyloid or tau species that accumulate with age in 3xTgAD mice (18).

Oestradiol and ER in female 3xTgAD mice

Epidemiological studies have shown a positive correlation between AD and the decrease of E_2 levels in women after menopause, suggesting a neuroprotective role for endogenous oestrogens in AD (7). Unlike in women, E_2 levels in serum and brain were unchanged with age in 3xTgAD and ntg mice. Female mice were sacrificed during pro-oestrus to ensure high serum E_2 levels, which ranged from 6.9 to 12.3 pg/ml, similar to previous reports (32,54). By contrast, a study reported serum E_2 levels of approximately 100 pg/ml in 6 month-old 3xTgAD female mice (8). The reason for this discrepancy is likely methodological because our stringent sample preparation using solid phase extraction and extensive washing very effectively removes substances that can interfere with the radioimmunoassay (31).

Despite the increased interest in measuring local E_2 concentrations in the brain of humans and other animals (7), the present study is the first report detailing baseline concentrations of E_2 in the cortex, hypothalamus, amygdala and hippocampus in both male and female 3xTgAD and ntg mice. Although brain E_2 concentrations were unchanged across ages in both sexes and both genotypes, similar to female APP23 mice (7), we found significant regional differences in E_2 concentrations. E_2 levels in these brain regions were greater than E_2 levels in serum, suggesting that E_2 is synthesised within these brain regions (55,56). The local synthesis of E_2 may be mediated by brain aromatase activity independent of peripheral E_2, which is a process that appears to be conserved across vertebrate species (34,35,57,58). Functionally, locally produced E_2 plays a key role in synapse maintenance and its alteration induces cognitive impairment (59). Taken together, our findings indicate that the local production of E_2 in the hippocampus in male and female 3xTgAD

mice was not impaired or stimulated by the age-related increase of plaque and tangle pathology.

Despite the fact that E_2 levels did not change with age or genotype, we found significant changes in the number of ERα and ERβ positive neurones in the hippocampus and medial amygdala in female mice. Specifically, the number of ERα- and ERβ-IR cells was significantly higher in young female than older female mice independent of genotype. Similarly, when the female cohorts were combined by age, there was also a decrease in ERα positive cell numbers in the female medial amygdala of 3xTgAD compared to female ntg mice. Although the functional consequences of reduced numbers of ER positive neurones are unclear, it could affect cellular genomic signalling triggered by E_2. On the other hand, a decrease in receptor number as well as loss of receptor affinity with age (60) may lead to a functional loss of oestrogenic neuroprotection with age.

A decrease in neuroprotection by E_2 may explain the increase in the number of 6E10-positive plaques in the hippocampus (present study) and amygdala that occur in females compared to male 3xTgAD mice (18), as well as increased 6E10 staining intensity in young females versus age-matched 3xTgAD male mice. It is noteworthy that ER deficits occur in the hippocampus and amygdala, regions associated with memory function. which are affected by decreased E_2 levels (61) and other hormones of the hypothalamic-pituitary-gonadal axis (62). Interestingly, ovariectomy impacts levels of soluble and insoluble Aβ in other AD transgenic mouse models, including the APP Tg2576, APP/PS1 (54) and 3xTgAD (8) mice. Moreover, *in vitro* and *in vivo* studies have shown that E_2 reduces brain Aβ concentrations (8,54,62), suggesting that sex steroid hormones protect against the development of AD neuropathology. Taken together, the lower numbers of ER in the CA1 hippocampal and medial amygdala nuclei and the age-related trend toward decreased testosterone levels may predispose female 3xTgAD mice to develop early and more accelerated plaque pathology compared to male mutant mice displaying elevated testosterone and no decrease in AR positive neurones.

Our data demonstrate for the first time that testosterone levels in the serum and brain increase with age in male 3xTgAD mice, without changes in AR-IR cell numbers in hippocampus and medial amygdala. This age-related increase in testosterone parallels an increase in intraneuroneal tau in AR-containing CA1 hippocampal neurones indicative of a probable interaction between tau and testosterone that may alter Aβ production. By contrast, E_2 concentrations in the brain and serum were unchanged with age, whereas ER-IR cell numbers were reduced in female mice, perhaps predisposing this sex to develop an accelerated Aβ pathology compared to male mutant mice, which may be neuroprotected by high testosterone levels. Furthermore, the present findings show increases in testosterone in male 3xTgAD, which are in conflict with the reduction found in aged male humans. This disconnection suggests that this transgenic mouse model of AD may not be appropriate for the study of age- or surgically-induced manipulation of sex steroids and their relationship with the onset of AD pathology. More research is needed to better characterise sex steroids in this and other transgenic models of AD pathogenesis before making translational conclusions to the human condition.

Acknowledgements

The authors thank Ms Michelle Doman, Ms Lily Yu and Ms Shadiyat Shoaga for their help with stereology and immunohistochemistry and Mr Sifeng Xu for help with the radioimmunoassays. NIA AG10668 (E.J.M.), NIA T32AG000257 (E.J.M.), Shapiro Foundation (E.J.M.), Canadian Institutes of Health Research Operating Grant (K.K.S.) and CIHR CGS-D Fellowship (M.D.T.) supported this work.

Received 25 April 2012,
revised 3 August 2012,
accepted 7 August 2012

References

1 Braak H, Braak E. Neuropathological stageing of Alzheimer-related changes. *Acta Neuropathol* 1991; **82**: 239–259.
2 Thal DR, Rub U, Orantes M, Braak H. Phases of A beta-deposition in the human brain and its relevance for the development of AD. *Neurology* 2002; **58**: 1791–1800.
3 Pike CJ, Carroll JC, Rosario ER, Barron AM. Protective actions of sex steroid hormones in Alzheimer's disease. *Front Neuroendocrinol* 2009; **30**: 239–258.
4 Craig MC, Maki PM, Murphy DG. The Women's Health Initiative Memory Study: findings and implications for treatment. *Lancet Neurol* 2005; **4**: 190–194.
5 Perez S, Sendera TJ, Kordower JH, Mufson EJ. Estrogen receptor alpha containing neurons in the monkey forebrain: lack of association with calcium binding proteins and choline acetyltransferase. *Brain Res* 2004; **1019**: 55–63.
6 Mitra SW, Hoskin E, Yudkovitz J, Pear L, Wilkinson HA, Hayashi S, Pfaff DW, Ogawa S, Rohrer SP, Schaeffer JM, McEwen BS, Alves SE. Immunolocalization of estrogen receptor beta in the mouse brain: comparison with estrogen receptor alpha. *Endocrinology* 2003; **144**: 2055–2067.
7 Yue X, Lu M, Lancaster T, Cao P, Honda S, Staufenbiel M, Harada N, Zhong Z, Shen Y, Li R. Brain estrogen deficiency accelerates Abeta plaque formation in an Alzheimer's disease animal model. *Proc Natl Acad Sci USA* 2005; **102**: 19198–19203.
8 Carroll JC, Rosario ER, Chang L, Stanczyk FZ, Oddo S, LaFerla FM, Pike CJ. Progesterone and estrogen regulate Alzheimer-like neuropathology in female 3xTg-AD mice. *J Neurosci* 2007; **27**: 13357–13365.
9 Carroll JC, Rosario ER, Villamagna A, Pike CJ. Continuous and cyclic progesterone differentially interact with estradiol in the regulation of Alzheimer-like pathology in female 3xTransgenic-Alzheimer's disease mice. *Endocrinology* 2010; **151**: 2713–2722.
10 Ramsden M, Nyborg AC, Murphy MP, Chang L, Stanczyk FZ, Golde TE, Pike CJ. Androgens modulate beta-amyloid levels in male rat brain. *J Neurochem* 2003; **87**: 1052–1055.
11 Rosario ER, Carroll J, Pike CJ. Testosterone regulation of Alzheimer-like neuropathology in male 3xTg-AD mice involves both estrogen and androgen pathways. *Brain Res* 2010; **1359**: 281–290.
12 McAllister C, Long J, Bowers A, Walker A, Cao P, Honda S, Harada N, Staufenbiel M, Shen Y, Li R. Genetic targeting aromatase in male amyloid precursor protein transgenic mice down-regulates beta-secretase (BACE1) and prevents Alzheimer-like pathology and cognitive impairment. *J Neurosci* 2010; **30**: 7326–7334.
13 Overk CR, Lu P-Y, Wang Y-T, Choi J, Shaw JW, Thatcher GR, Mufson EJ. Effects of aromatase inhibition versus gonadectomy on hippocampal complex amyloid pathology in triple transgenic mice. *Neurobiol Dis* 2012; **45**: 479–487.
14 Oddo S, Caccamo A, Shepherd JD, Murphy MP, Golde TE, Kayed R, Metherate R, Mattson MP, Akbari Y, LaFerla FM. Triple-transgenic model

of Alzheimer's disease with plaques and tangles: intracellular Abeta and synaptic dysfunction. *Neuron* 2003; **39**: 409–421.
15 Oddo S, Caccamo A, Kitazawa M, Tseng BP, LaFerla FM. Amyloid deposition precedes tangle formation in a triple transgenic model of Alzheimer's disease. *Neurobiol Aging* 2003; **24**: 1063–1070.
16 Caccamo A, Oddo S, Billings LM, Green KN, Martinez-Coria H, Fisher A, LaFerla FM. M1 receptors play a central role in modulating AD-like pathology in transgenic mice. *Neuron* 2006; **49**: 671–682.
17 Overk CR, Kelley CM, Mufson EJ. Brainstem Alzheimer's-like pathology in the triple transgenic mouse model of Alzheimer's disease. *Neurobiol Dis* 2009; **35**: 415–425.
18 Oh KJ, Perez SE, Lagalwar S, Vana L, Binder L, Mufson EJ. Staging of Alzheimer's pathology in triple transgenic mice: a light and electron microscopic analysis. *Int J Alzheimers Dis* 2010; **15**: pii:780102.
19 Rosario ER, Carroll JC, Oddo S, LaFerla FM, Pike CJ. Androgens regulate the development of neuropathology in a triple transgenic mouse model of Alzheimer's disease. *J Neurosci* 2006; **26**: 13384–13389.
20 Taves MD, Schmidt KL, Ruhr IM, Kapusta K, Prior NH, Soma KK. Steroid concentrations in plasma, whole blood and brain: effects of saline perfusion to remove blood contamination from brain. *PLoS One* 2010; **5**: e15727.
21 Goldman JM, Murr AS, Cooper RL. The rodent estrous cycle: characterization of vaginal cytology and its utility in toxicological studies. *Birth Defects Res B Dev Reprod Toxicol* 2007; **80**: 84–97.
22 McNamara KM, Harwood DT, Simanainen U, Walters KA, Jimenez M, Handelsman DJ. Measurement of sex steroids in murine blood and reproductive tissues by liquid chromatography-tandem mass spectrometry. *J Steroid Biochem Mol Biol* 2010; **121**: 611–618.
23 Perez SE, He B, Muhammad N, Oh KJ, Fahnestock M, Ikonomovic MD, Mufson EJ. Cholinotrophic basal forebrain system alterations in 3xTg-AD transgenic mice. *Neurobiol Dis* 2010; **41**: 338–352.
24 Perez SE, Chen EY, Mufson EJ. Distribution of estrogen receptor alpha and beta immunoreactive profiles in the postnatal rat brain. *Brain Res Dev Brain Res* 2003; **145**: 117–139.
25 Lu SF, McKenna SE, Cologer-Clifford A, Nau EA, Simon NG. Androgen receptor in mouse brain: sex differences and similarities in autoregulation. *Endocrinology* 1998; **139**: 1594–1601.
26 Paxinos G, Franklin K, eds. *The Mouse Brain in Stereotaxic Coordinates*. London: Academic Press, 2001:
27 Perez SE, Lazarov O, Koprich JB, Chen EY, Rodriguez-Menendez V, Lipton JW, Sisodia SS, Mufson EJ. Nigrostriatal dysfunction in familial Alzheimer's disease-linked APPswe/PS1DeltaE9 transgenic mice. *J Neurosci* 2005; **25**: 10220–10229.
28 Mufson EJ, Lavine N, Jaffar S, Kordower JH, Quirion R, Saragovi HU. Reduction in p140-TrkA receptor protein within the nucleus basalis and cortex in Alzheimer's disease. *Exp Neurol* 1997; **146**: 91–103.
29 Moeller ML, Dimitrijevich SD. A new strategy for analysis of phenotype marker antigens in hollow neurospheres. *J Neurosci Methods* 2004; **139**: 43–50.
30 Gundersen HJ, Jensen EB, Kieu K, Nielsen J. The efficiency of systematic sampling in stereology–reconsidered. *J Microsc* 1999; **193**: 199–211.
31 Taves MD, Ma C, Heimovics SA, Saldanha CJ, Soma KK. Measurement of steroid concentrations in brain tissue: methodological considerations. *Front Endocrinol* 2011; **2**: 39.
32 Haisenleder DJ, Schoenfelder AH, Marcinko ES, Geddis LM, Marshall JC. Estimation of estradiol in mouse serum samples: evaluation of commercial estradiol immunoassays. *Endocrinology* 2011; **152**: 4443–4447.
33 Newman AE, Chin EH, Schmidt KL, Bond L, Wynne-Edwards KE, Soma KK. Analysis of steroids in songbird plasma and brain by coupling solid phase extraction to radioimmunoassay. *Gen Comp Endocrinol* 2008; **155**: 503–510.
34 Charlier TD, Newman AE, Heimovics SA, Po KW, Saldanha CJ, Soma KK. Rapid effects of aggressive interactions on aromatase activity and oestradiol in discrete brain regions of wild male white-crowned sparrows. *J Neuroendocrinol* 2011; **23**: 742–753.
35 Charlier TD, Po KW, Newman AE, Shah AH, Saldanha CJ, Soma KK. 17beta-Estradiol levels in male zebra finch brain: combining Palkovits punch and an ultrasensitive radioimmunoassay. *Gen Comp Endocrinol* 2010; **167**: 18–26.
36 Shughrue PJ, Merchenthaler I. Distribution of estrogen receptor beta immunoreactivity in the rat central nervous system. *J Comp Neurol* 2001; **436**: 64–81.
37 Merchenthaler I, Lane MV, Numan S, Dellovade TL. Distribution of estrogen receptor alpha and beta in the mouse central nervous system: in vivo autoradiographic and immunocytochemical analyses. *J Comp Neurol* 2004; **473**: 270–291.
38 Jean-Faucher C, Berger M, de Turckheim M, Veyssiere G, Jean C. Developmental patterns of plasma and testicular testosterone in mice from birth to adulthood. *Acta Endocrinol* 1978; **89**: 780–788.
39 Dong Q, Salva A, Sottas CM, Niu E, Holmes M, Hardy MP. Rapid glucocorticoid mediation of suppressed testosterone biosynthesis in male mice subjected to immobilization stress. *J Androl* 2004; **25**: 973–981.
40 Luria A, Morisseau C, Tsai HJ, Yang J, Inceoglu B, De Taeye B, Watkins SM, Wiest MM, German JB, Hammock BD. Alteration in plasma testosterone levels in male mice lacking soluble epoxide hydrolase. *Am J Physiol Endocrinol Metab* 2009; **297**: E375–E383.
41 Lacombe A, Lelievre V, Roselli CE, Muller JM, Waschek JA, Vilain E. Lack of vasoactive intestinal peptide reduces testosterone levels and reproductive aging in mouse testis. *J Endocrinol* 2007; **194**: 153–160.
42 Case LK, Toussaint L, Moussawi M, Roberts B, Saligrama N, Brossay L, Huber SA, Teuscher C. Chromosome y regulates survival following murine coxsackievirus b3 infection. *G3* 2012; **2**: 115–121.
43 Hampl R, Ivanyi P, Starka L. Testosterone and testosterone binding in murine plasma. *Steroidologia* 1971; **2**: 113–120.
44 Bartke A. Increased sensitivity of seminal vesicles to testosterone in a mouse strain with low plasma testosterone levels. *J Endocrinol* 1974; **60**: 145–148.
45 Brouillette J, Rivard K, Lizotte E, Fiset C. Sex and strain differences in adult mouse cardiac repolarization: importance of androgens. *Cardiovasc Res* 2005; **65**: 148–157.
46 Hogervorst E, Williams J, Budge M, Barnetson L, Combrinck M, Smith AD. Serum total testosterone is lower in men with Alzheimer's disease. *Neuro Endocrinol Lett* 2001; **22**: 163–168.
47 Davidoff MS, Middendorff R, Pusch W, Muller D, Wichers S, Holstein AF. Sertoli and Leydig cells of the human testis express neurofilament triplet proteins. *Histochem Cell Biol* 1999; **111**: 173–187.
48 Sternbach H. Age-associated testosterone decline in men: clinical issues for psychiatry. *Am J Psychiatry* 1998; **155**: 1310–1318.
49 Moffat SD, Zonderman AB, Metter EJ, Kawas C, Blackman MR, Harman SM, Resnick SM. Free testosterone and risk for Alzheimer disease in older men. *Neurology* 2004; **62**: 188–193.
50 Gandy S, Almeida OP, Fonte J, Lim D, Waterrus A, Spry N, Flicker L, Martins RN. Chemical andropause and amyloid-beta peptide. *J Am Med Assoc* 2001; **285**: 2195–2196.
51 Yao M, Nguyen TV, Rosario ER, Ramsden M, Pike CJ. Androgens regulate neprilysin expression: role in reducing beta-amyloid levels. *J Neurochem* 2008; **105**: 2477–2488.
52 Papasozomenos S, Shanavas A. Testosterone prevents the heat shock-induced overactivation of glycogen synthase kinase-3 beta but not of cyclin-dependent kinase 5 and c-Jun NH2-terminal kinase and concomitantly abolishes hyperphosphorylation of tau: implications for Alzheimer's disease. *Proc Nat Acad Sci USA* 2002; **99**: 1140–1145.

53 Hammond J, Le Q, Goodyer C, Gelfand M, Trifiro M, LeBlanc A. Testosterone-mediated neuroprotection through the androgen receptor in human primary neurons. *J Neurochem* 2001; **77**: 1319–1326.
54 Zheng H, Xu H, Uljon SN, Gross R, Hardy K, Gaynor J, Lafrancois J, Simpkins J, Refolo LM, Petanceska S, Wang R, Duff K. Modulation of A(beta) peptides by estrogen in mouse models. *J Neurochem* 2002; **80**: 191–196.
55 Barker JM, Galea LA. Sex and regional differences in estradiol content in the prefrontal cortex, amygdala and hippocampus of adult male and female rats. *Gen Comp Endocrinol* 2009; **164**: 77–84.
56 Garcia-Segura LM, Wozniak A, Azcoitia I, Rodriguez JR, Hutchison RE, Hutchison JB. Aromatase expression by astrocytes after brain injury: implications for local estrogen formation in brain repair. *Neuroscience* 1999; **89**: 567–578.
57 Azcoitia I, Sierra A, Veiga S, Garcia-Segura LM. Aromatase expression by reactive astroglia is neuroprotective. *Ann NY Acad Sci* 2003; **1007**: 298–305.
58 Yague JG, Munoz A, de Monasterio-Schrader P, Defelipe J, Garcia-Segura LM, Azcoitia I. Aromatase expression in the human temporal cortex. *Neuroscience* 2006; **138**: 389–401.
59 Fester L, Prange-Kiel J, Zhou L, Blittersdorf BV, Bohm J, Jarry H, Schumacher M, Rune GM. Estrogen-regulated synaptogenesis in the hippocampus: sexual dimorphism in vivo but not in vitro. *J Steroid Biochem Mol Biol* 2012; **131**: 24–29.
60 Chakraborty TR, Gore AC. Aging-related changes in ovarian hormones, their receptors, and neuroendocrine function. *Exp Biol Med* 2004; **229**: 977–987.
61 Woolley CS, Gould E, Frankfurt M, McEwen BS. Naturally occurring fluctuation in dendritic spine density on adult hippocampal pyramidal neurons. *J Neurosci* 1990; **10**: 4035–4039.
62 Meethal SV, Smith MA, Bowen RL, Atwood CS. The gonadotropin connection in Alzheimer's disease. *Endocrine* 2005; **26**: 317–326.

